tive exponential dependence on $n(\omega)$, identical in both equations, produces an opposing effect which tends to nullify the change arising from the factors of $[n(\omega)\beta - 1]^{1/2}$. The result is an effective change in the force ratio F_x/F_z by a factor $(\frac{2}{3})^{1/2}$ and a consequent 20% reduction in the total deflection angle.

[16]See Ref. 10, p. 21.

[17]See Ref. 10, p. 27.

PHYSICAL REVIEW A VOLUME 5, NUMBER 3 MARCH 1972

Relativistic Hartree-Fock-Slater Calculations for Arbitrary Temperature and Matter Density*

Balazs F. Rozsnyai

Lawrence Radiation Laboratory, University of California, Livermore, California 94550

(Received 19 July 1971)

An algorithm is presented to calculate electronic levels and the equation of state of atoms suitable for arbitrary matter density and temperature. The self-consistent-field treatment starts with relativistic Thomas-Fermi-Dirac model in the iterative procedure. The Fermi statistics and the central-field approximation are maintained, giving an average atom representation. The broadening of upper electronic levels into bands is taken into account in a simple approximation. Calculations are presented for the Fe^{26} and Rb^{37} atoms at several temperatures and matter densities.

I. INTRODUCTION

The Thomas-Fermi (TF) and Thomas-Fermi-Dirac (TFD) statistical models of atom were extended to finite temperatures by Feynman, Metropolis, and Teller,[1] and by Cowan and Ashkin,[2] respectively, some years ago. Since then these models have been widely used to calculate atomic properties at high temperature and pressure. It is generally believed that in the region of high temperature and/or pressure, the TFD model gives a reasonably accurate electron potential. This potential in turn can be used as a basis to treat the atom in a more quantum-mechnical way by solving the single-electron wave equation for the bound states. The inclusion of shell effects in the TF model in this matter was used by Carson, Mayers, and Stibbs to calculate stellar opacities.[3] The same principle was applied by Zink[4,5] to obtain the energy of partially ionized matter using an analytical potential in place of the exact TFD potential. He appropriately labeled the model as the Thomas-Fermi-shell (TFS) model. We can recognize the TFS model as the first iteration in a Hartree-Fock (HF) or Hartree-Fock-Slater (HFS) self-consistent-field scheme in which the TFD potential is used as the beginning. At low or moderately high temperatures, the TFS model may or may not be adequate, depending on the actual physical properties that one wishes to calculate. The first purpose of this paper is to study this uncertainty by a comprehensive self-consistent-field program. Since no HFS calculations are known to the author for temperatures when the atomic electrons are partially degenerate, the author believes that this paper fills a gap in an area of considerable interest. The second purpose is to formulate the self-consistent model for atoms in a manner suitable for finite matter density calculations. This is done by making allowance for the splitting of upper electronic levels into bands in a somewhat crude approximation. The importance of band splitting at high matter density is important in connection with the accurate treatment of level broadenings. The exchange due to the Pauli principle is taken into account in the free-electron or plane-wave approximation as is done in the TFD and HFS models. The Fermi statistics and the central-field approximation are maintained throughout the calculations. Since relativistic effects may be important in the case of heavy elements, the relativistic formulation is maintained. It is assumed that the reader is familiar with the HF and TF theories and, therefore, detailed derivations are avoided.

II. REVIEW OF RELATIVISTIC TFD THEORY

The relativistic expression for the electron density in the TF approximation is given by[6]

$$\rho(r) = \frac{8\pi}{h^3c^3} \int_{\epsilon_0(r)}^{\infty} \frac{\{[\epsilon - V(r)]^2 - m^2c^4 - [rV'(r)]^2\}^{1/2}}{e^{(\epsilon-\mu)/kT} + 1} [\epsilon - V(r)]\, d\epsilon \,, \tag{1a}$$

where c is the velocity of light, h the Planck constant, m the electron mass, T the temperature in degrees Kelvin, k the Boltzmann constant, $V(r)$ the potential energy function for the electron, assumed to be spherically symmetrical, and $V'(r)$ its derivative with respect to r, which is the distance from the center of the atom. The chemical potential or Fermi level μ is determined by the normalization condition

$$4\pi \int_0^{R_0} \rho(r) r^2 dr = N \ ,$$

where N is the number of electrons. R_0 is the radius of a spherical volume containing the atom; the magnitude of R_0 is determined by the matter density. The lower limit of the integral ϵ_0 is determined by the condition that the expression in curly braces in (1a) must not be less than zero, which yields

$$\epsilon_0(r) = V(r) + q(R) \ ,$$

where

$$q(r) = \{m^2c^4 + [rV'(r)]^2\}^{1/2} \ . \tag{1b}$$

Expression (1a) for the electron density can be written in a more familiar form by making the substitutions $\epsilon \to \epsilon + \epsilon_0$ and $\mu \to \mu - mc^2$ and by assuming that $kT \ll mc^2$. In this case we can expand the radical in (1a) in a power series, and after some straightforward manipulation we obtain

$$\rho(r) = \frac{4\pi}{h^3c^3} [2kTq(r)]^{3/2} \left[I_{1/2}(z) + \frac{5}{4} \frac{kT}{q(r)} I_{3/2}(z) + \frac{7}{32} \frac{k^2T^2}{q^2(r)} I_{5/2}(z) + 0 \left(\frac{kT}{q(r)} \right)^3 \right] , \tag{1c}$$

where

$$z = z(r) = \frac{\mu - V(r) + mc^2 - q(r)}{kT} \tag{1d}$$

and the I's represent the Fermi-Dirac integrals given by

$$I_\nu(z) = \int_0^\infty \frac{t^\nu}{e^{(t-z)} + 1} \, dt \ .$$

In formula (1c) the function $q(r)$ plays the role of a relativistic mass correction. Neglecting the term rV' and retaining only the $I_{1/2}$ term, one obtains from (1c) the usual nonrelativistic TF electron density. It is noteworthy that the relativistic effect is manifested in two ways, first through the term rV', which is important near the center and exists at any temperature, and second through the series expansion which is temperature dependent.

The potential energy V can be written as

$$V(r) = -Ze^2/r + V_c(r) + V_{ex}(r) + V_{corr}(r) \ . \tag{2}$$

The first term in (2) is due to the nucleus of charge Z; the second is the classical electron-electron interaction, which must satisfy the Poisson equation with the proper boundary conditions,

$$\nabla^2 V_c(r) = -4\pi\rho e^2 \ , \tag{3}$$

where e is the elementary charge. The third and fourth terms in (2) correspond to the exchange and correlation, respectively,[7] and both of them are approximated as local potentials in the free-electron approximation. At zero temperature the exchange potential in terms of the electron density is given by[8] (in atomic units)

$$V_{ex}^0(r) = -\tfrac{3}{2} (3/\pi)^{1/3} \rho^{1/3}(r) \ , \tag{4a}$$

where the superscript 0 indicates the zero-temperature case. For temperatures sufficiently high so that the electron gas can be considered as Maxwellian, we have (see Appendix A)

$$V_{ex}^M(r) = -\pi\rho(r)/kT \ , \tag{4b}$$

where the superscript M indicates the Maxwellian distribution. For intermediate temperatures, we interpolate between the zero- and high-temperature limits and use[9]

$$V_{ex}(r) = [1 - \lambda^2(r)] V_{ex}^0(r) + \lambda^2(r) V_{ex}^M(r) \ , \qquad 0 \le \lambda \le 1 \tag{4c}$$

$$V_{ex}(r) = V_{ex}^M(r) \ , \qquad \lambda \ge 1$$

where

$$\lambda(r) = 2k\,T/(3\pi^2)^{2/3} \rho^{2/3}(r) \ .$$

The correlation potential is taken into account in the zero-temperature limit as follows:

$$V_{corr} = 0.0622 \ln r_s - 0.096 + 0.0049 r_s \ln r_s \ , \qquad r_s \le 1 \tag{5a}$$

$$V_{corr} = -\frac{0.112\,94}{\rho^{1/3} + 0.1216} \rho^{1/3} \ , \qquad r_s > 1 \tag{5b}$$

where $r_s = (3/4\pi)^{1/3} \rho^{-1/3}$. Equation (5a) is the high-density approximation of the correlation potential with the first two terms due to Gell-Mann and Brueckner[10] and the last term due to Dubois.[11] Equation (5b) is the low-density approximation of the correlation potential given by Wigner.[12]

Equations (1a)–(5b) represent the formulas of the relativistic TFD model in which the correlation is also included. These equations can be solved by fast digital computers, and the TFD potential can be used as a suitable beginning in an HFS interative procedure.

III. REVIEW OF HFS MODEL

It is assumed that the reader is familiar with the HF and HFS models applied to the ground state of an isolated atom or ion. It is well known that

the low excited states and different angular-momentum states for open-shell configurations can be calculated with sufficient accuracy from the data of a ground-state HFS calculation by the perturbation method. For higher excited states, the perturbation treatment using ground-state energy levels and wave functions is no longer feasible, and one must apply the HF method for the excited configurations. In the high-temperature case, the number of possible configurations is enormous, and therefore one must resort to some sort of averaging treatment. A plausible way to do this is based on the assumption that the atomic electrons occupy the single-particle levels according to Fermi statistics. This leads to a fictitious atom with noninteger occupational numbers, and this average atom is assumed to represent a close approximation to the canonical average.[13] This is the basic assumption in Refs. 3–5 and also in this paper.

In the average-atom approximation, the radial density of bound electrons is given by

$$\rho_b(r) = \frac{1}{4\pi} \sum_{nl} \frac{2(2l+1)}{e^{(\epsilon_{nl}-\mu)/kT}+1} \left| \frac{R_{nl}(r)}{r} \right|^2 , \qquad (6a)$$

where the summation is over all the bound levels and ϵ_{nl} is the single-particle energy with principal and angular-momentum quantum numbers n and l, respectively. If spin-orbit splitting is taken into account, then the factor $2(2l+1)$ is replaced by $2j+1$, where $j = l \pm \frac{1}{2}$ and the index j is added everywhere to n and l. R_{nl} is the radial part of the single-particle wave function given by

$$\psi_{nlm}(r, \theta\phi) = \frac{R_{nl}(r)}{r} Y_{\phi m}(\theta\phi) ,$$

$$\int_0^{R_0} R_{nl}^2(r)\, dr = 1 ,$$

where $Y_{\phi m}$ represents the spherical harmonics. R_{nl} satisfies the usual relativistic or nonrelativistic radial equation with the potential $V(r)$. The usual boundary conditions that R_{nl} must satisfy, and which in turn determine ϵ_{nl}, are

$$R_{nl}(0) = 0 \qquad (7a)$$

and

$$R_{nl}(R_0) = 0 \qquad (7b)$$

or

$$\frac{d}{dr}\left[\frac{R_{nl}(r)}{r}\right] = 0 \quad \text{at } r = R_0 , \qquad (7c)$$

where R_0, as in Sec. II, is the radius of the sphere containing the atom. In the case of a finite matter density, R_0 is finite; one can satisfy either (7b) or (7c), yielding two different values for ϵ_{nl}, with the one corresponding to (7b) being the larger. In the case of homonuclear diatomic molecules this type of splitting corresponds to the "gerade" and "ungerade" or bonding and antibonding type of molecular electronic levels. In the case of bulk matter, when an atom is surrounded by many neighbors, one can assume that the two energies corresponding to boundary conditions (7b) and (7c) are the upper and lower edges, respectively, of a band. This assumption can be justified by the following considerations: Let us assume that the matter is of finite density, in which case the wave functions extend over the whole region occupied by the matter, and let us assume that the central-field approximation is still valid within the radius R_0 of each atom. In this case the radial part of the lowest-energy wave function with principal and angular-momentum quantum numbers n and l can have no more nodes than $n-l-1$ at each center. This wave function must be symmetric with respect to an elementary translation so condition (7c) must hold.[14] By similar arguments the highest possible energy ϵ_{nl} belongs to a wave function with R_{nl} having an additional node between each two centers, in which case the condition (7b) is satisfied. It should be noted that, for an isolated atom, when R_0 is infinitely large the bandwidths reduce to zero because the boundary conditions (7b) and (7c) for the bound states are satisfied simultaneously, giving a discrete level ϵ_{nl}.[15]

In the absence of any detailed knowledge about the structure of the matter, the distribution of states within a band is taken to be equal to that of free electrons, which is a frequent approximation in solid-state physics. Accordingly, the density of states in the nl band, denoted by $g_{nl}(\epsilon)$, has to be proportional to $\epsilon^{1/2}$, where ϵ is the energy measured from the lower limit of the band. Also, the normalization condition

$$\int_0^{\Delta\epsilon_{nl}} g_{nl}(\epsilon)\, d\epsilon = 2(2l+1)$$

has to be satisfied, where $\Delta\epsilon_{nl} = \epsilon_{nl}^{II} - \epsilon_n^I$, ϵ_{nl}^{II} and ϵ_{nl}^I being the upper and lower limits of the nl band, respectively. These requirements can be satisfied by

$$g_{nl}(\epsilon) = \frac{3(2l+1)}{(\Delta\epsilon_{nl})^{3/2}} \epsilon^{1/2} . \qquad (8a)$$

When spin-orbit splitting is taken into account, Eq. (8a) must be replaced by

$$g_{nlj}(\epsilon) = \frac{3}{2} \frac{2j+1}{(\Delta\epsilon_{nlj})^{3/2}} \epsilon^{1/2} . \qquad (8b)$$

Taking into account the band-splitting as described above, the radial density of bound electrons is given by

$$\rho_b(r)$$

$$= \frac{1}{4\pi} \sum_{nl} \left(\int_0^{\Delta\epsilon_{nl}} \frac{g_{nl}(\epsilon)}{e^{(\epsilon_{nl}^{I} + \epsilon - \mu)/kT} + 1} \left| \frac{R_{nl\delta}(r)}{r} \right|^2 d\epsilon \right) , \tag{6b}$$

where $\delta = \epsilon_{nl}^{I}$ and $R_{nl\delta}$ is now a radial function with the energy parameter between ϵ_{nl}^{I} and ϵ_{nl}^{II}, and *no* boundary conditions are imposed at R_0. Since the wave function $R_{nl\delta}$ is calculated only at the band limits with boundary condition (7b) or (7c), formula (6b) can be approximated by

$$\rho_b(r) \approx \frac{1}{4\pi} \sum_{nl} \frac{N_{nl}^{I} |R_{nl}^{I}(r)|^2 + N_{nl}^{II} |R_{n}^{II}(r)|^2}{r^2} , \tag{6c}$$

where R_{nl}^{I} and R_{nl}^{II} are the radial wave function with boundary conditions (7c) and (7b), respectively, and the numbers N_{nl}^{I} and N_{nl}^{II} are determined by the equations

$$\begin{aligned} N_{nl}^{I} + N_{nl}^{II} &= N_{nl} , \\ N_{nl}^{I} \epsilon_{nl}^{I} + N_{nl}^{II} \epsilon_{nl}^{II} &= N_l \bar{\epsilon}_{nl} , \end{aligned} \tag{6d}$$

where N_{nl} is the band population and $\bar{\epsilon}_{nl}$ is the band energy average given by

$$N_{nl} = \int_0^{\Delta\epsilon_{nl}} \frac{g_{nl}(\epsilon)}{e^{(\epsilon_{nl}^{I} + \epsilon - \mu)/kT} + 1} \, d\epsilon , \tag{6e}$$

$$N_{nl} \bar{\epsilon}_{nl} = N_l \epsilon_{nl}^{I} + \int_0^{\Delta\epsilon_{nl}} \frac{g_{nl}(\epsilon)\, \epsilon}{e^{(\epsilon_{nl}^{I} + \epsilon - \mu)/kT} + 1} \, d\epsilon . \tag{6f}$$

The density of free electrons $\rho_f(r)$ can be calculated in the TF or TFD approximation using formula (1a) with ϵ_0, the lower limit of the integral, properly changed. The condition that determines ϵ_0 now is that the single-particle energy (including the rest energy) $\epsilon \geq q(R)$. This leads to a formula completely analogous to (1c) with the Fermi-Dirac integrals I_ν being replaced by the incomplete Fermi-Dirac integrals $I_\nu^{x_0}(z)$, where

$$X_0 = X_0(r) = -V(r)/kT , \tag{9}$$

z is given by (1d), and

$$I_\nu^{x_0}(z) = \int_{x_0}^{\infty} \frac{t^\nu}{e^{t-z}+1} \, dt .$$

The free- and bound-electron densities together, when integrated over the volume containing the atom, must yield the total number of electrons. Since the bound electrons are treated by wave mechanics, the normalization condition for the total electron density yields a different chemical potential μ than the TF or TFD method. Naturally, this difference is significant at low temperatures when there are many bound electrons. Having de-

TABLE I. Energy levels and populations in Fe^{26} at $kT = 0$ at different matter densities. $D_0 = 7.85$ g/cm^3.

	$D = 0.1D_0$			$D = D_0$			$D = 20D_0$	
	ϵ_{nlj} (a.u.)	N_{nlj}		ϵ_{nlj} (a.u.)	N_{nlj}		ϵ_{nlj} (a.u.)	N_{nlj}
$1s_{1/2}$	−261.79	2.000 0	$1s_{1/2}$	−260.51	2.000 0	$1s_{1/2}$	−253.75	2.000 0
$2s_{1/2}$	−30.915	2.000 0	$2s_{1/2}$	−30.578	2.000 0	$2s_{1/2}$	−24.862	2.000 0
$2p_{1/2}$	−26.907	2.000 0	$2p_{1/2}$	−26.602	2.000 0	$2p_{1/2}$	−20.727	2.000 0
$2p_{3/2}$	−26.450	4.000 0	$2p_{3/2}$	−26.141	4.000 0	$2p_{3/2}$	−20.277	4.000 0
$3s_{1/2}$	−3.375 1	2.000 0	$3s_{1/2}$	−3.248 7	2.000 0	$3s_{1/2}^{I}$	−2.3688	0.240 09
$3p_{1/2}$	−2.161 4	2.000 0	$3p_{1/2}$	−2.051 7	2.000 0	$3s_{1/2}^{II}$	>0	
$3p_{3/2}$	−2.104 9	4.000 0	$3p_{3/2}$	−1.996 3	4.000 0	μ	8.6583	
$4s_{1/2}^{I}$	−0.174 06	0.529 29	$4s_{1/2}^{II}$	−0.182 44	0.156 43			
$3d_{3/2}$	−0.159 91	4.000 0	$3d_{3/2}^{I}$	−0.120 85	3.137 43			
$3d_{5/2}$	−0.154 72	3.221 91	$3d_{5/2}^{I}$	−0.116 30	4.706 14			
$4s_{1/2}^{II}$	−0.139 25	0.248 79	$3d_{3/2}^{II}$	+0.004 35				
			$4s_{1/2}^{II}$	+0.075 814	0			
$4p_{1/2}^{I}$	−0.037 49		$3d_{5/2}^{II}$	+0.108 3				
$4p_{3/2}^{I}$	−0.035 89	0	μ	−0.100 59				
$4p_{1/2}^{II}$								
$4p_{3/2}^{II}$	>0							
μ	−0.154 72							

TABLE II. Energy levels and populations in Rb^{37} at $kT=0$ at different matter densities. $D_0=1.532$ g/cm^2.

	$D=0.5D_0$			$D=D_0$			$D=20D_0$	
	ϵ_{nlj} (a.u.)	N_{nlj}		ϵ_{nlj} (a.u.)	N_{nlj}		ϵ_{nlj} (a.u.)	N_{nlj}
$1s_{1/2}$	−562.24	2.000 0	$1s_{1/2}$	−561.39	2.000 0	$1s_{1/2}$	−556.56	2.000 0
$2s_{1/2}$	−76.405	2.000 0	$2s_{1/2}$	−76.263	2.000 0	$2s_{1/2}$	−74.165	2.000 0
$2p_{1/2}$	−69.561	2.000 0	$2p_{1/2}$	−69.482	2.000 0	$2p_{1/2}$	−67.561	2.000 0
$2p_{3/2}$	−67.392	4.000 0	$2p_{3/2}$	−67.307	4.000 0	$2p_{3/2}$	−65.346	4.000 0
$3s_{1/2}$	−11.801	2.000 0	$3s_{1/2}$	−11.779	2.000 0	$3s_{1/2}$	−10.352	2.000 0
$3p_{1/2}$	−9.237 6	2.000 0	$3p_{1/2}$	−9.289 7	2.000 0	$3p_{1/2}$	−7.910 8	2.000 0
$3p_{3/2}$	−8.955 4	4.000 0	$3p_{3/2}$	−8.947 6	4.000 0	$3p_{3/2}$	−7.575 9	4.000 0
$3d_{3/2}$	−4.572 9	4.000 0	$3d_{3/2}$	−4.568 5	4.000 0	$3d_{3/2}$	−3.220 9	4.000 0
$3d_{5/2}$	−4.515 5	6.000 0	$3d_{5/2}$	−4.510 8	6.000 0	$3d_{5/2}$	−3.163 7	6.000 0
$4s_{1/2}$	−1.384 5	2.000 0	$4s_{1/2}$	−1.385 9	2.000 0	$4s^{I}_{1/2}$	−1.022 9	1.724 1
$4p_{1/2}$	−0.784 27	2.000 0	$4p_{1/2}$	−0.787 53	2.000 0	$4p^{I}_{1/2}$	−0.436 93	0.321 69
$4p_{3/2}$	−0.748 62	4.000 0	$4p_{3/2}$	−0.751 88	4.000 0	$4p^{I}_{3/2}$	−0.403 31	0.643 39
$5s^{I}_{1/2}$	−0.157 34	0.621 55	$5s^{I}_{1/2}$	−0.171 05	0.621 60	$4s^{II}_{1/2}$		
$5p^{I}_{1/2}$	−0.066 96	0	$4d^{I}_{3/2}$	−0.065 31		$4p^{II}_{1/2}$	>0	
$5p^{I}_{3/2}$	−0.063 50	0	$4d^{I}_{5/2}$	−0.069 17	0	$4p^{II}_{3/2}$		
$5s^{II}_{1/2}$	−0.057 47	0.378 45	$5p^{I}_{1/2}$	−0.063 33		μ	0.879 25	
$4d^{I}_{3/2}$	−0.057 47		$5p^{II}_{3/2}$	−0.058 46	0			
$4d^{II}_{5/2}$	−0.057 42		$5s^{II}_{1/2}$	−0.003 29	0.376 40			
$4d^{II}_{3/2}$	−0.009 6	0	$4d^{II}_{3/2}$	+0.007 78				
$4d^{II}_{5/2}$	−0.007 7		$4d^{II}_{5/2}$	+0.010 05				
$5p^{II}_{1/2}$	>0		$5p^{II}_{1/2}$					
$5p^{II}_{3/2}$	>0		$5p^{II}_{3/2}$	>0				
μ	−0.094 482		μ	−0.065 45				

termined the total electron density, we can calculate the electron potential including exchange and correlation as described in Sec. II, and the iterative procedure can be carried forward until the desired accuracy is achieved.

IV. CALCULATIONS

A computer program was written to solve the relativistic TFD problem for atoms as described in Sec. II, and the TFD potential was used as the input of an HFS program. The relativistic single-particle equations for the bound states were solved by using the two-component Dirac equation in the central field and eliminating the small component. The bound- and free-electron densities were calculated as described in Sec. III, and the iterative procedure was carried out until the maximum deviation in the potential in two successive iteration was less than 1%. In addition to the quantities indicated in Secs. II and III, total electronic energy, electron entropy, and electron pressure at the boundary were also calculated. The formulas for the latter quantities are summarized in Appendix B.

The calculations were performed for the Fe^{26} and Rb^{37} atoms at several temperatures up to $kT = 5\times10^4$ eV and at several matter densities. The data are given in atomic units where the unit energy is 27.204 eV and the unit distance is 0.5292×10^{-8} cm. Only those data are presented that the author thinks reflect the main features of the calculations, and even so they seem rather abundant. For this reason, the results of the TFD calculation that are the starting points of the program are not presented. For the Fe^{26} atom the TFD data agree with those of Ref. 2 in the nonrelativistic limit. Tables I–IV summarize the data concerning the relativistic single-electron levels in the self-consistent potentials of the Fe^{26} and Rb^{37} atoms at $kT = 0$ and 100 eV with some of the matter densities. In the tables D is the matter density (g/cm^3), D_0 is the normal density and ϵ_{nlj} and N_{nlj} are the single-

TABLE III. Energy levels and populations in Fe^{26} at $kT = 100$ eV at different matter densities.

	$D = 0.1D_0$			$D = D_0$			$D = 20D_0$	
	ϵ_{nlj} (a.u.)	N_{nlj}		ϵ_{nlj} (a.u.)	N_{nlj}		ϵ_{nlj} (a.u.)	N_{nlj}
$1s_{1/2}$	−273.43	2.000 0	$1s_{1/2}$	−266.021	2.000 0	$1s_{1/2}$	−254.22	2.000 0
$2s_{1/2}$	−42.075 3	1.998 5	$2s_{1/2}$	−35.746	1.999 0	$2s_{1/2}$	−25.272	1.999 7
$2p_{1/2}$	−38.197	1.995 8	$2p_{1/2}$	−31.831	1.997 2	$2p_{1/2}$	−21.152	1.999 2
$2p_{3/2}$	−37.730	3.990 4	$2p_{3/2}$	−31.363	3.993 7	$2p_{3/2}$	−20.700	3.998 2
$3s_{1/2}$	−11.341	0.481 3	$3s_{1/2}$	−6.523 7	0.850 61	$3s^{I}_{1/2}$	−1.533 2	0.261 18
$3p_{1/2}$	−10.125	0.370 89	$3p_{1/2}$	−5.283 1	0.691 15	$3p^{I}_{1/2}$	−0.093 41	0.001 818
$3p_{3/2}$	−10.025	0.725 57	$3p_{3/2}$	−5.196 4	1.361 1	$3p^{II}_{3/2}$	−0.035 22	0.003 629
$3s_{3/2}$	−8.242 9	0.480 27	$3d_{3/2}$	−3.232 9	0.928 58	$3s^{II}_{1/2}$	>0	
$3d_{5/2}$	−8.224 9	0.717 31	$3d_{5/2}$	−3.218 4	1.388 6	$3p^{II}_{1/2}$	>0	
$4s_{1/2}$	−3.630 2	0.074 900	$4s^{I}_{1/2}$	−0.532 83	0.970 87	$3p^{II}_{3/2}$	>0	
$4p_{1/2}$	−3.169 0	0.066 357	$4p^{I}_{1/2}$	−0.186 00	0.044 176	μ	7.534 01	
$4p_{3/2}$	−3.139 4	0.131 69	$4p^{I}_{3/2}$	−0.174 38	0.088 104			
$4d_{3/2}$	−2.458 8	0.110 04	$4s^{II}_{1/2}$	−0.111 53	0.141 48			
$4d_{5/2}$	−2.453 5	0.164 83	$4p^{II}_{1/2}$	>0				
$4f_{5/2}$	−1.842 4	0.140 18	$4p^{II}_{3/2}$	>0				
$4f_{7/2}$	−1.840 9	0.186 83	μ	−7.630 2				
$5s_{1/2}$	−0.976 39	0.037 100						
$5p_{1/2}$	−0.776 88	0.035 174						
$5p_{3/2}$	−0.765 72	0.070 139						
$5d_{3/2}$	−0.473 41	0.064 865						
$5d_{5/2}$	−0.471 47	0.097 246						
$5f_{5/2}$	−0.212 11	0.090 721						
$5f_{7/2}$	−0.211 55	0.120 94						
$6s^{I}_{1/2}$	−0.078 69	0.005 86						
$6s^{II}_{1/2}$	>0							
μ	−15.564 5							

particle energies and populations, respectively. When band splitting occurs in the upper states, superscripts I and II are used in the spectroscopic notations for the lower and upper limits of the bands, respectively. In the latter case the numbers in the column N_{nlj} are understood to be N^{I}_{nlj} or N^{II}_{nlj} as given by formulas (6d)–(6f), and their sums are the band populations. The Fermi level μ is also given. The energy levels at zero temperature and at low matter densities agree with those of Herman and Skillman.[16] The bandwidths calculated at zero temperature in the crude approximation adopted in this paper cannot agree with those of more detailed solid-state calculations. However, the data obtained by this method are not bad. In the case of the Fe^{26} atom at $kT = 0$ and $D = D_0$, the calculated widths of the $4s$, $3d_{3/2}$, and $3d_{5/2}$ bands are 0.26, 0.13, and 0.22 a.u., respectively. These values compare rather favorably with those obtained by Gandel'man[17]: about 0.3 a.u. for the $4s$ band and about 0.2, 0.1, and ~0 for the $3d$ $M = 2$, $M = 1$, and $M = 0$ bands, respectively. It is known from solid-state calculations that the $4s$ band is completely filled, whereas Table I at $D = D_0$ shows only 0.16 $4s$ electrons. This is an obvious shortcoming of the central-field approximation. In the case of Rb^{37} atom, the $5s$ bandwidth at $D = D_0$ and $kT = 0$ is 0.17 a.u., from Table II, in reasonable agreement with the value of about 0.13 a.u., obtained by Ham,[18] and the band is half-filled. The single-electron levels for the Fe^{26} and Rb^{37} atoms at $kT = 100$ eV at different matter densities are shown in Tables III and IV, respectively. At higher temperatures, when the

TABLE IV. Energy levels and populations in Rb^{37} at $kT = 100$ eV at different matter densities.

	$D = 0.5D_0$			$D = D_0$			$D = 20D_0$	
	ϵ_{nlj} (a.u.)	N_{nlj}		ϵ_{nlj} (a.u.)	N_{nlj}		ϵ_{nlj} (a.u.)	N_{nlj}
$1s_{1/2}$	−575.63	2.000 0	$1s_{1/2}$	−573.72	2.000 0	$1s_{1/2}$	−561.01	2.000 0
$2s_{1/2}$	−89.702	2.000 0	$2s_{1/2}$	−88.497	2.000 0	$2s_{1/2}$	−78.465	2.000
$2p_{1/2}$	−82.955	2.000 0	$2p_{1/2}$	−81.809	2.000 0	$2p_{1/2}$	−71.907	2.000
$2p_{3/2}$	−80.774	4.000 0	$2p_{3/2}$	−79.623	4.000 0	$2p_{3/2}$	−69.684	4.000
$3s_{1/2}$	−22.732	1.746 7	$3s_{1/2}$	−21.766	1.767 64	$3s_{1/2}$	−13.375	1.867 2
$3p_{1/2}$	−20.276	1.559 6	$3p_{1/2}$	−19.323	1.585 66	$3p_{1/2}$	−10.946	1.758 3
$3p_{3/2}$	−19.855	3.037 1	$3p_{3/2}$	−18.905	3.093 3	$3p_{3/2}$	−10.566	3.470 3
$3d_{3/2}$	−15.753	2.032 6	$3d_{3/2}$	−14.785	2.105 9	$3d_{3/2}$	−6.297 7	2.688 8
$3d_{5/2}$	−15.674	3.016 5	$3d_{5/2}$	−14.707	3.126 7	$3d_{5/2}$	−6.226 0	4.007 3
$4s_{1/2}$	−7.099 1	0.178 67	$4s_{1/2}$	−6.385 6	0.203 27	$4s^{I}_{1/2}$	−1.084 3	0.251 82
$4p_{1/2}$	−6.202 6	0.142 74	$4p_{1/2}$	−5.500 4	0.163 30	$4s^{II}_{1/2}$	−0.414 52	0.364 37
$4p_{3/2}$	−6.086 4	0.277 25	$4p_{3/2}$	−5.387 8	0.317 56	$4p^{I}_{1/2}$	−0.409 19	0.154 78
$4d_{3/2}$	−4.661 2	0.192 44	$4d_{3/2}$	−3.971 4	0.221 65	$4p^{I}_{3/2}$	−0.359 41	0.306 66
$4d_{5/2}$	−4.640 1	0.287 09	$4d_{5/2}$	−3.951 0	0.330 74	$4p^{II}_{1/2}$	>0	
$4f_{5/2}$	−3.260 1	0.200 22	$4f_{5/2}$	−2.568 6	0.231 06	$4p^{II}_{3/2}$	>0	
$4f_{7/2}$	−3.255 4	0.266 64	$4f_{7/2}$	−2.564 3	0.307 74	μ	3.657 98	
$5s_{1/2}$	−2.402 3	0.053 22	$5s_{1/2}$	−1.885 9	0.064 387			
$5p_{1/2}$	−2.024 7	0.048 150	$5p_{1/2}$	−1.523 7	0.058 520			
$5p_{3/2}$	−1.981 04	0.095 191	$5p_{3/2}$	−1.483 5	0.115 81			
$5d_{3/2}$	−1.387 49	0.081 287	$5d_{3/2}$	−0.912 41	0.099 558			
$5d_{5/2}$	−1.379 40	0.121 67	$5d_{5/2}$	−0.905 15	0.149 05			
$5f_{5/2}$	−0.844 44	0.104 64	$5f_{5/2}$	−0.363 17	0.129 06			
$5f_{7/2}$	−0.812 63	0.139 45	$5f_{7/2}$	−0.361 69	0.172 01			
$6s_{1/2}$	−0.554 94	0.032 540	$6s^{I}_{1/2}$	−0.285 34	0.016 65			
$6p^{I}_{1/2}$	−0.399 42	0.012 925	$6p^{I}_{3/2}$	−0.147 41	0.074 47			
$5g_{7/2}$	−0.388 01	0.124 47	$6s^{II}_{1/2}$	−0.179 58	0.024 78			
$5g_{9/2}$	−0.387 60	0.155 57	$6p^{I}_{1/2}$	−0.157 78	0.037 33			
$6p^{I}_{3/2}$	−0.378 75	0.024 747	$6p^{II}_{1/2}$	>0				
$6p^{II}_{1/2}$	−0.366 02	0.018 603	$6p^{II}_{3/2}$	>0				
$6p^{II}_{3/2}$	−0.347 84	0.037 026	μ	−14.396				
$6d^{I}_{3/2}$	−0.144 45	0.023 121						
$6d^{I}_{5/2}$	−0.142 09	0.034 660						
$6d^{II}_{3/2}$	−0.070 07	0.034 489						
$6d^{II}_{5/2}$	−0.066 57	0.051 686						
μ	−15.634							

atom becomes partially ionized, a number of new levels appear which are partially or almost completely vacant and very much resemble the levels of the hydrogenic sequence. However, because of the screening by the free electrons, hydrogenic degeneracy is never reached. These upper states have large Bohr radii; consequently they are very sensitive to change in matter density. In Figs. 1–4 the quantity $4\pi r^2\rho(r)$ is shown at $D = D_0$ and $10D_0$ and at $kT = 0$ and 100 eV. At high matter den-

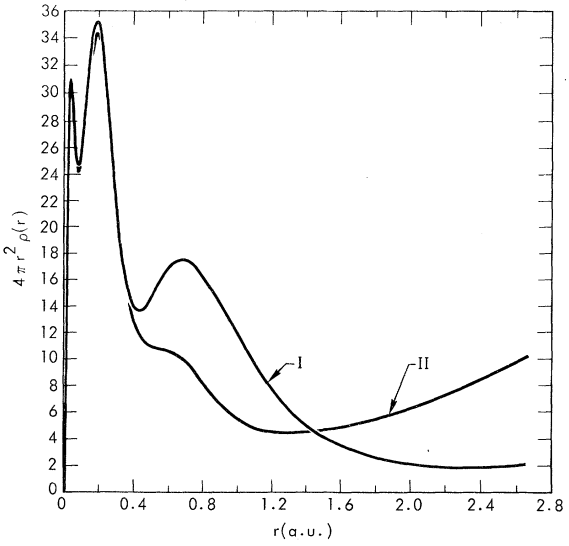

FIG. 1. $4\pi r^2\rho(r)$, where $\rho(r)$ is the self-consistent electron density of the Fe^{26} atom at normal matter density (7.85 g/cm^3) at $kT=0$ (I) and 100 eV (II).

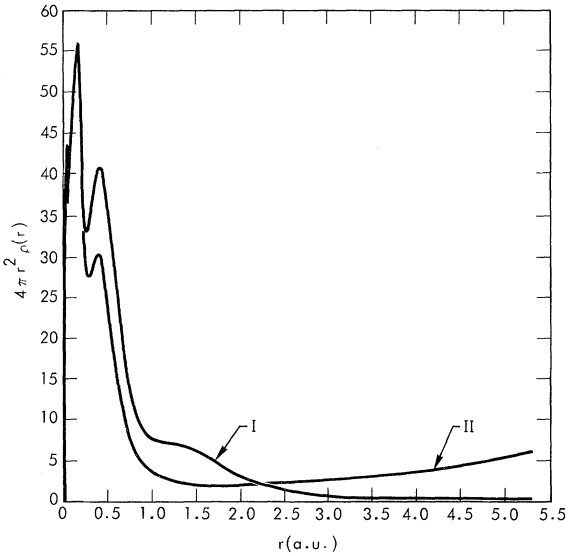

FIG. 3. $4\pi r^2\rho(r)$ of the Rb^{37} atom at normal matter density (1.532 g/cm^3) at $kT=0$ (I) and 100 eV (II).

sity and/or high temperature, the tails of the curves become nearly parabolic as a result of the free-electron density.[19] In Figs. 5–8 the quantity $rV(r) = -Z^*(r)$ is shown. $Z^*(r)$ can be regarded as a position-dependent effective nuclear charge. In the case of rigorous exact calculations, Z^* must be equal to $Z-N+1$ at the boundary R_0.[20]

Some properties of the whole atom are summarized in Fig. 9–17. Figures 9 and 10 show the total electronic energy above the self-consistent ground-state energy of the isolated atom at different matter densities and temperatures for the Fe^{26} and Rb^{37} atoms, respectively. The dashed lines indicate the results of the first iteration which can be regarded as the TFS results. For the Rb^{37} atom, the TFS energy curves at $kT=0$ and 10 eV show a rather erratic behavior, which is smoothed out for the self-consistent solution[21]; therefore they are not shown. At higher temperatures and matter densities, the TFS results are very close to the self-consistent HFS results. Figures 11 and 12 show TS, where S is the entropy of the electron

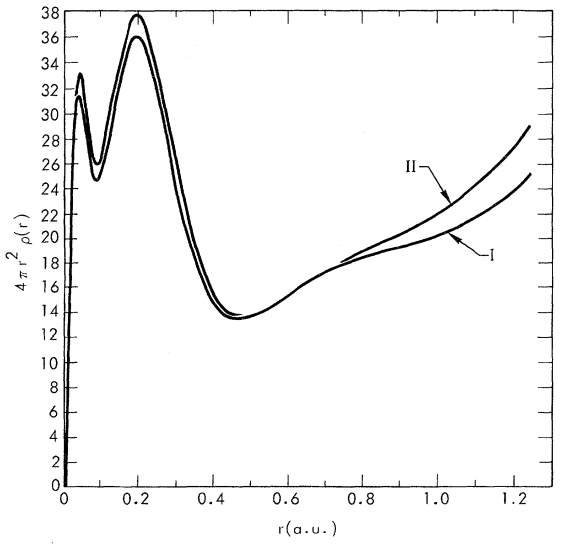

FIG. 2. $4\pi r^2\rho(r)$ of the Fe^{26} atom at ten times normal matter density (78.5 g/cm^3) at $kT=0$ (I) and 100 eV (II).

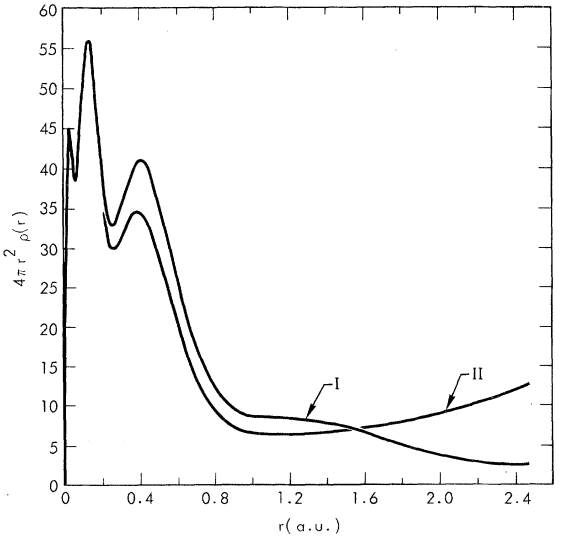

FIG. 4. $4\pi r^2\rho(r)$ of the Rb^{37} atom at ten times normal matter density (15.32 g/cm^3) at $kT=0$ (I) and 100 eV (II).

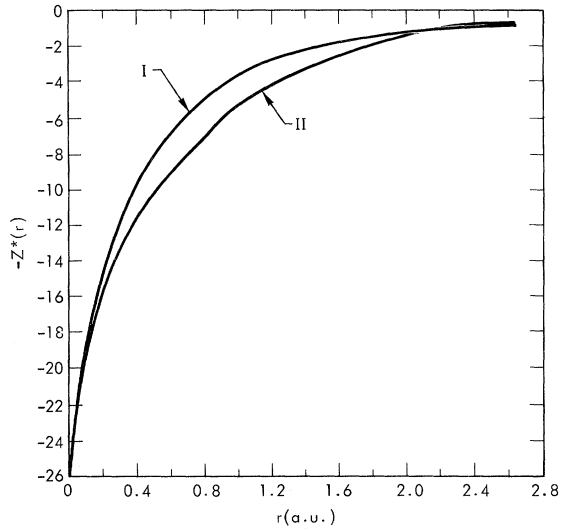

FIG. 5. $rV(r) = -Z^*(r)$ of the Fe^{26} atom at normal matter density (7.85 g/cm^3) at $kT = 0$ (I) and 100 eV (II). $V(r)$ is the self-consistent potential including exchange and correlation.

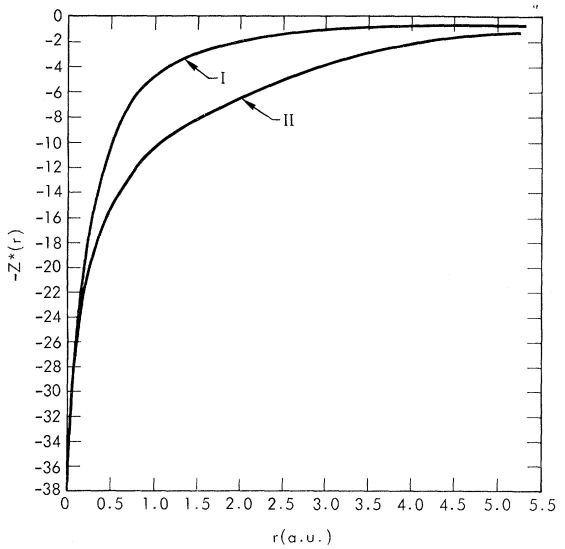

FIG. 7. $-Z^*(r)$ of the Rb^{37} atom at normal matter density at $kT = 0$ (I) and 100 eV (II).

gas, and Figs. 13 and 14 show the logarithm of the electron pressure at the boundary R_0 as a function of matter density at different temperatures. Figure 15 shows the electron pressure at the boundary R_0 of the Rb^{37} atom in the low-temperature region close to the ground state at different matter densities. The self-consistent-field pressures at low matter density show some unexpected minima with respect to the temperature between $kT = 0.5$ and 1 eV. This is due to the fact that electrons are lifted from the 5s band into the 4d band and the 4d wave functions extend outward less than the 5s wave functions. This feature does not appear in the results of the first TFS iteration, because there the 5s and 4d bands are farther apart. Figures 16 and 17 show the number of free electrons as a function of matter density at different temperatures.

APPENDIX A: EXCHANGE INTERACTION IN FREE-ELECTRON GAS

The Coulomb exchange between two plane waves confined in a volume Ω is given by

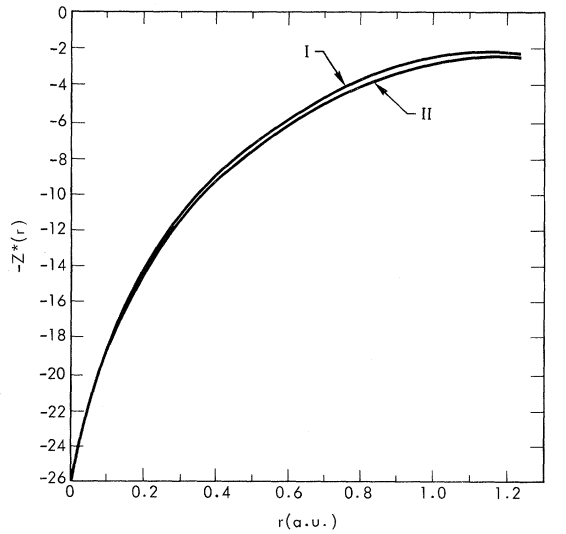

FIG. 6. $-Z^*(r)$ of the Fe^{26} atom at ten times normal matter density at $kT = 0$ (I) and 100 eV (II).

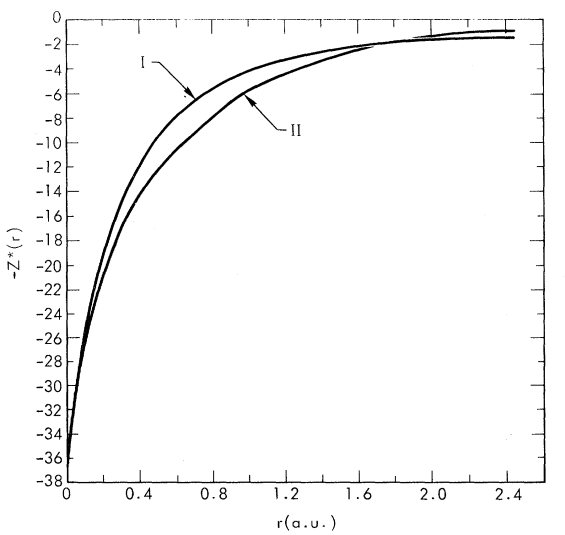

FIG. 8. $-Z^*(r)$ of the Rb^{37} atom at ten times normal matter density at $kT = 0$ (I) and 100 eV (II).

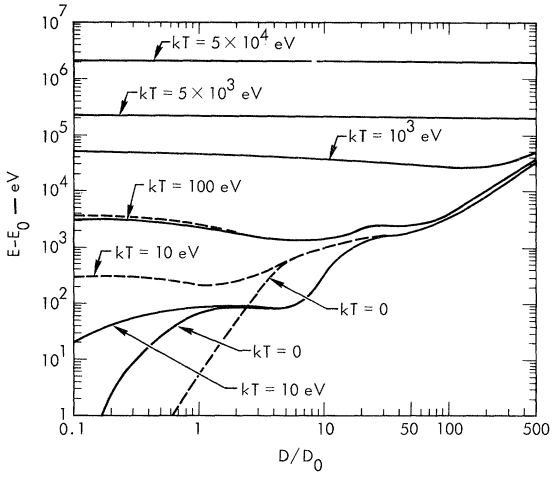

FIG. 9. Electronic energy of the Fe^{26} atom above the ground-state self-consistent energy of the isolated atom ($E_0 = -3.3970 \times 10^4$ eV) as a function of matter density at different temperatures. Solid lines, HFS results; dashed lines, TFS results.

$$\epsilon_{jl} = -h^2e^2/\Omega\pi \left| \vec{P}_j - \vec{P}_l \right|^2 , \tag{A1}$$

where h is the Planck constant, e the elementary charge, and $\vec{P}_j$ and $\vec{P}_l$ the two momentum vectors. The number of l electrons with spin parallel to j in the solid cone $2\pi p_l^2 dp_l \sin\theta\, d\theta$ is given by

$$dn_l = \frac{2\pi\Omega}{h^3} \frac{p_l^2 dp_l \sin\theta\, d\theta}{e^{(p_l^2/2m - \mu)/kT} + 1} ,$$

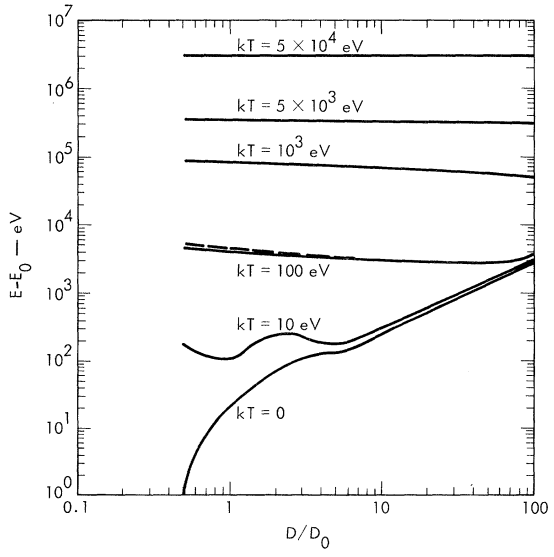

FIG. 10. Electronic energy of the Rb^{37} atom above the ground-state self-consistent energy of the isolated atom ($E_0 = -7.963\,56 \times 10^4$ eV) as a function of matter density at different temperatures. Dashed line, TFS results at 100 eV.

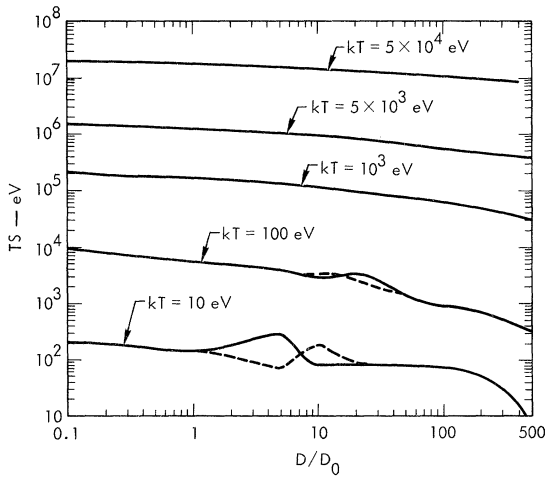

FIG. 11. *TS* of the Fe^{26} atom as a function of matter density at different temperatures. Solid lines, HFS results; dashed lines TFS results.

so we have

$$\sum_l \epsilon_{jl} \approx -\frac{2e^2}{h} \int_0^\infty \frac{p_l^2 dp_l}{e^{(p_l^2/2m - \mu)/kT} + 1} \times \int_0^\pi \frac{\sin\theta\, d\theta}{p_l^2 + p_j^2 - 2p_j p_l \sin\theta} .$$

The integral with respect to θ yields a factor

$$\frac{1}{p_j p_l} \ln \frac{p_j + p_l}{|p_j - p_l|} ,$$

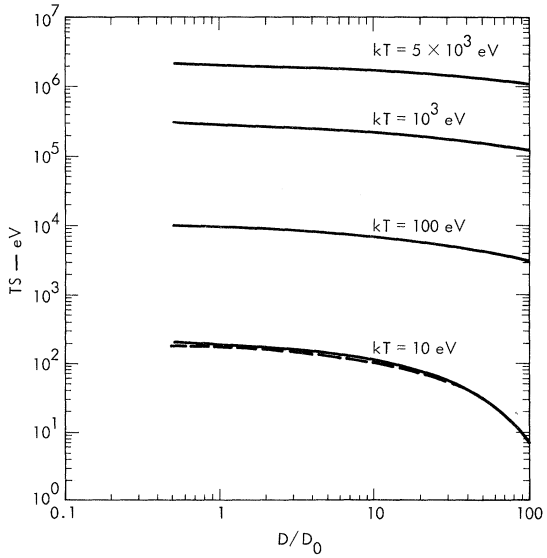

FIG. 12. *TS* of the Rb^{37} atom as a function of matter density at different temperatures. Solid lines, HFS results; dashed lines, TFS results.

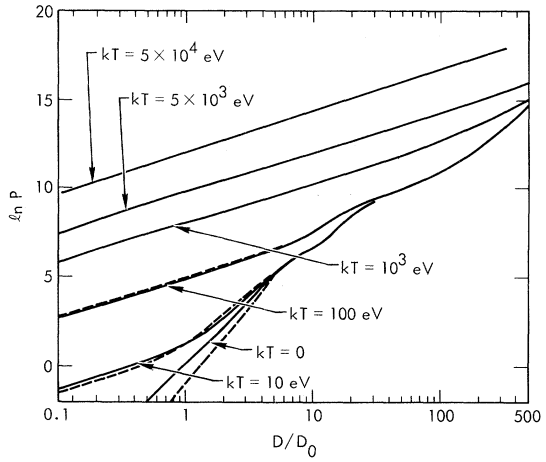

FIG. 13. Logarithm of the electron pressure P (in megabars) of the Fe^{26} atom at the boundary as a function of matter density at different temperatures. Solid lines, HFS results; dashed lines, TFS results.

and we have

$$\frac{1}{2}\sum_{j,l}{}'' \epsilon_{jl} \approx -\frac{4\pi e^2}{h^4}\,\Omega \times \int_0^\infty \int_0^\infty \frac{p_l p_j \ln[(p_j+p_l)/|p_j-p_l|]\,dp_l\,dp_j}{(e^{(p_l^2/2m-\mu)/kT}+1)\,(e^{(p_j^2/2m-\mu)/kT}+1)}\,, \tag{A2}$$

where the $\uparrow\uparrow$ indicates the summation over parallel spins only, so that the total exchange energy is twice (A2). In the zero-temperature limit, the double integral in (A2) yields $\frac{1}{2}p_F{}^4$, where $p_F = (2m\mu)^{1/2}$ is the Fermi momentum; hence the total exchange energy is given by

$$E_{ex}^0 = -\frac{4\pi e^2}{h^4}\,p_F{}^4\,\Omega$$

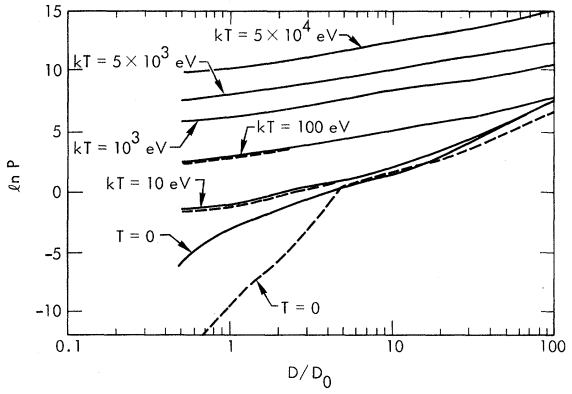

FIG. 14. Logarithm of the electron pressure P (in megabars) of the Rb^{37}atom at the boundary as a function of matter density at different temperatures. Solid lines, TFS results.

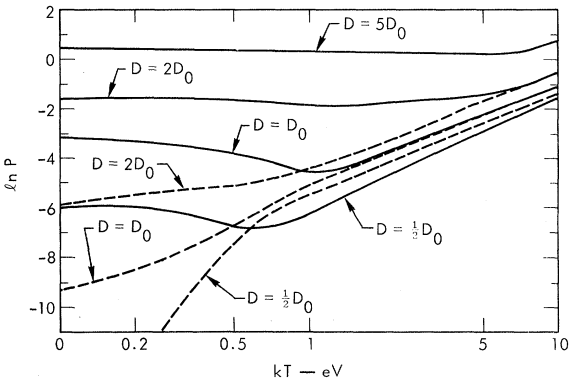

FIG. 15. Logarithm of the electron pressure P (in megabars) of the Rb^{37} atom at the boundary in the low-temperature region at different densities. Solid lines, HFS results; dashed lines, TFS results.

$$= -\frac{3}{4}\left(\frac{3}{\pi}\right)^{1/2} e^2\Omega\rho^{4/3}\,, \tag{A3}$$

where the superscript 0 stands for the zero temperature. In (A3) the relation $p_F = \frac{1}{2}h(3/\pi)^{1/3}\rho^{1/3}$ was used, where ρ is the electron density. In the case of very high temperature, when the electron gas can be considered Maxwellian, the double integral in (A2) can be written as

$$e^{2\mu/kT}(2mkT)^2\,I\,,$$

where

$$I = \int_0^\infty \int_0^\infty xy\,e^{-x^2-x^2}\ln\left(\frac{x+y}{|x-y|}\right)dxdy = \tfrac{1}{8}\pi\,.$$

The normalization condition requires that

$$e^{2\mu/kT} = \tfrac{1}{4}\rho^2(h^2/2mkT\pi)^3\,,$$

and after collecting all the terms we get for the total exchange energy

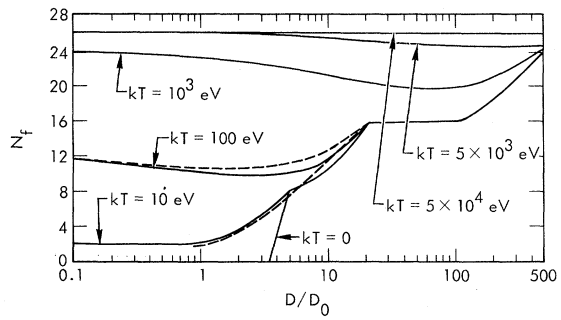

FIG. 16. Number of free electrons in the Fe^{26} atom as a function of matter density at different temperatures. Solid lines, HFS results; dashed lines, TFS results.

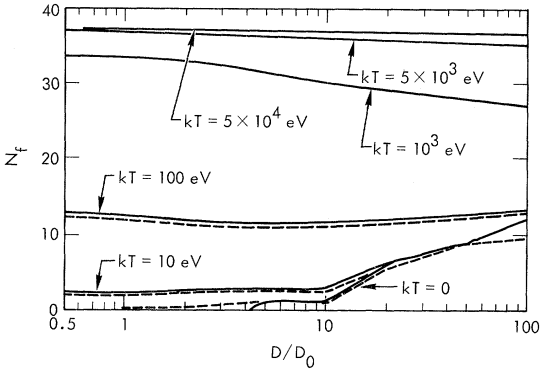

FIG. 17. Number of free electrons in the Rb^{37} atom as a function of matter density at different temperatures. Solid lines, HFS results; dashed lines, TFS results.

$$E_{ex}^{M} = -\frac{e^2\Omega}{4}\,\frac{h^2}{2mkT\pi}\,\rho^2 = -\frac{\hbar^2e^2}{m}\,\frac{\pi\rho^2}{2kT} = -e^4a_0\,\frac{\pi\rho^2}{2kT}\,\Omega\,, \tag{A4}$$

where a_0 is the Bohr radius, and the superscript M stands for the Maxwellian case. We define the exchange potential by

$$E_{ex} = \tfrac{1}{2}\int V_{ex}(r)\,\rho(r)\,d^3r\,,$$

which yields

$$V_{ex}^{0} = -\tfrac{3}{2}\,(3/\pi)^{1/2}\,\rho^{1/2}(r)\,e^2 \tag{A5}$$

and

$$V_{ex}^{M} = -\,[\pi\rho(r)/kT]e^4a_0 \tag{A6}$$

or formulas (4a) and (4b), respectively, if kT and ρ are given in atomic units. For intermediate temperatures one has to somehow interpolate between the two limits in a reasonable manner. A possible choice for the parameter of the interpolation is the ratio of the thermal energy to the zero-point Fermi energy given by

$$\lambda = 2kT/(3\pi^2)^{2/3}\rho^{2/3}\,.$$

If an interpolation formula,

$$V_{ex} = [1-\lambda^n]\,V_x^0 + \lambda^n V_x^M\,,$$

is used, n must be larger than 1 because of the dependence of V_x^M on $1/kT$. In this paper a simple quadratic interpolation was used as given by formula (4c).

APPENDIX B: FORMULAS

In this section the formulas used to calculate the total electronic energy, electron pressure at the boundary, and electron entropy are summarized.

The total electronic energy is given by

$$E = \sum_{nl} N_{nl}\,\bar{\epsilon}_{nl} + 4\pi\int_0^{R_0}\rho_\epsilon(r)\,r^2\,dr - 2\pi\int_0^{R_0} V_c(r)\rho(r)\,r^2dr\,, \tag{B1}$$

where the summation is over all the bound states, and the band populations N_{nl} and band-energy averages $\bar{\epsilon}_{nl}$ are given by (6e) and (6f), respectively. The $\rho_\epsilon(r)$ stands for the single-particle energy density of the free electrons and is given by

$$\rho_\epsilon(r) = \frac{8\pi}{h^3c^3}\,k^2T^2\int_{X_0(r)}^{\infty}\frac{[k^2T^2x^2+2xkTq(r)]^{1/2}\,[kTx+q(r)]\,[x-X_0(r)]}{e^{x-z(r)}+1}\,dx\,, \tag{B2}$$

where $X_0(r)$, $q(r)$, and $z(r)$ are given by formulas (9), (1b), and (1d), respectively. The electron pressure at the boundary is given by

$$P = \frac{8\pi}{3h^3c^3}\,[2kTq(R_0)]^{3/2}\,kT\left(I_{3/2}[z(R_0)] + \frac{3}{4}\,\frac{kT}{q(R_0)}\,I_{5/2}[z(R_0)] + \frac{3}{32}\,\frac{k^2T^2}{q^2(R_0)}\,I_{7/2}[z(R_0)]\right)\,. \tag{B3}$$

Formula (B3) is the relativistic Thomas-Fermi formula for the electron pressure. The quantum effect of the bound states is taken into account by inserting the HFS self-consistent values of the chemical potential μ and $V(R_0)$ into the expression for z. For the quantity TS, where S is the electron entropy, the following formula was used:

$$TS = \sum_{nl}\left(N_{nl}\,\bar{\epsilon}_{nl} - kT\int_0^{\Delta\epsilon_{nl}} g_{nl}(\epsilon)\ln\frac{e^{(\epsilon_{nl}^I+\epsilon-\mu)/kT}}{e^{(\epsilon_{nl}^I+\epsilon-\mu)/kT}+1}\,d\epsilon\right) - N\mu + 4\pi\int_0^{R_0}\rho_s(r)\,r^2dr\,, \tag{B4}$$

where the function $\rho_s(r)$ is given by

$$\rho_s(r) = k^2T^2\,\frac{8\pi}{h^3c^3}\int_{X_0(r)}^{\infty}[k^2T^2x^2+2kTq(r)]^{1/2}[kTx+q(r)]\{\ln[e^{x-z(r)}+1]-x+z(r)\}dx\,. \tag{B5}$$

Equations (B4) and (B5) result from a straightforward derivation from the basic formula for the entropy,

$$S = -k \int [n_i \ln n_i + (1-n_i)\ln(1-n_i)] ,$$

where the integral stands for summation of discrete levels and integration over continuum levels and

$$n_i = (e^{(\epsilon_i - \mu)/kT} + 1)^{-1} .$$

---

*Work performed under the auspices of the U. S. Atomic Energy Commission.

[1]R. P. Feynman, N. Metropolis, and E. Teller, Phys. Rev. 75, 1561 (1949).

[2]R. D. Cowan and J. Ashkin, Phys. Rev. 105, 144 (1957).

[3]T. R. Carson, D. F. Mayers, and D. W. N. Stibbs, Monthly Notices Roy. Astron. Soc. 140, 483 (1968).

[4]J. W. Zink, Phys. Rev. 176, 279 (1968).

[5]J. W. Zink, Astrophys. J. 162, 145 (1970).

[6]See P. Gombas, in *Encyclopedia of Physics* (Springer, Berlin, 1956), Vol. 36, p. 162.

[7]The correlation and exchange potentials are defined as $\frac{1}{2}\int V_{\text{ex, corr}}\rho d^3r = E_{\text{ex, corr}}$ (total exchange or correlation energy).

[8]J. C. Slater, *Quantum Theory of Atomic Structure* (McGraw-Hill, New York, 1960), Vol. II, p. 14.

[9]An exact treatment of the exchange in the plane-wave approximation valid at any temperature is given in Ref. 2. That leads to a rather complicated integral equation for the electron distribution in the momentum and coordinate space. Since the effect of the exchange in general is small compared to the direct Coulomb interaction, the author thinks that the present approximation of the exchange does not introduce much error. It should also be noted that the formulas used for the exchange and correlation parts of the potential are nonrelativistic.

[10]M. Gell-Mann and K. A. Brueckner, Phys. Rev. 106, 364 (1957).

[11]D. F. Dubois, Ann. Phys. (N.Y.) 7, 174 (1949); 8, 24 (1959).

[12]E. P. Wigner, Trans. Faraday Soc. 34, 678 (1938).

[13]No detailed analysis of this problem is known to the author. For heavy atoms it is reasonable to assume that the two averages are close. For light elements the differences may be significant. A comparison was made between the energy of the average atom and the energy average via detailed configuration accounting for helium at $KT = 5$ eV. The difference between the two methods was about 20%.

[14]The boundary condition (7c) is the Wigner-Seitz condition for the lower limit of an s band [see C. Kittel, *Quantum Theory of Solids* (Wiley, New York, 1963)]. The estimation of bandwidths by using conditions (7b) and (7c) is appropriate for s bands. For bands belonging to higher angular-momentum states, they are crude because directional properties are averaged out. For this reason it can be assumed that this type of treatment of the bandwidths is appropriate in the case of structureless fluids.

[15]For an isolated atom the conditions (7b) and (7c) simply reduce to the well-known condition that $R_{nl}(r) \to 0$ as $r \to \infty$. This condition was used in Ref. 3 and is valid only for low-density matter.

[16]F. Herman and S. Skillman, *Atomic Structure Calculations* (Prentice-Hall, Englewood Cliffs, N. J., 1963).

[17]G. M. Gandel'man, Zh. Eksperim. i Teor. Fiz. 43, 131 (1962) [Sov. Phys. JETP 16, 94 (1963)]. The quoted numbers are not very accurate because they were obtained from Gandel'man's graphs.

[18]F. S. Ham, Phys. Rev. 128, 82 (1962).

[19]It is customary to assume (Refs. 3–5) that the free-electron density $\rho_f(r)$ is uniform. This is not a very accurate assumption, and the TF or TFD treatment of free electrons clearly shows it. The effect of this difference on the upper-level positions is considerable.

[20]The discrepancy at R_0 is due to the fact that the Slater approximation for the exchange [Eqs. (4a)–(4c)] and the Gell-Mann–Brueckner approximations for the correlation are not exact. In some calculations (Refs. 3 and 5), where correlation is not taken into account, the self-field of an electron is taken into account by multiplying the electron-electron interaction potential V_c by $(N-1)/N$. This assures that at R_0 Z^* equals $Z-N+1$ as it should. The difference between that method and the one adopted in this paper is noticeable only at very low matter densities.

[21]Since the total electronic energy is computed with a relative accuracy of about 2–3%, the author is not certain whether the erratic behavior of the TFS energy of the Rb^{37} atom at low temperature is due to this uncertainty or to the fact that at different densities the TFS results approximate the HFS results with different accuracies.